Analytical Methods

RSC Publishing

PAPER

View Article Online
View Journal | View Issue

Cite this: *Anal. Methods*, 2013, **5**, 2727

Metabolomic study on the hepatoprotective effects of modified Sinisan using ultra-performance liquid chromatography/electrospray ionization quadruple time-of-flight mass spectrometry coupled with pattern recognition approach

Xiao-Wei Du,†[a] Xiao-Li Wang,†[a] De-You Jiang,[b] Nai-Zhi Geng,[c] Shuo-Xin Zhang,[c] Yuan-Yuan Zhou[a] and Cheng-Gang Liu*[b]

Metabolomics, the global analysis of small molecules in a biological system in a holistic context, has played increasingly important roles in studies on the potential mechanisms of drugs. Modified Sinisan (MSNS), a traditional Chinese medicine, has showed good clinical efficacy in the treatment of liver injury, and its mechanism remains unclear. The present study was undertaken to explore the metabolomic characters of liver injury induced by dimethylnitrosamine and the therapeutic effects of MSNS. The study utilized ultra-performance liquid chromatography/electrospray ionization quadruple time-of-flight mass spectrometry (UPLC/ESI-Q-TOF-MS) in positive electrospray ionization combined with pattern recognition approach including principal component analysis (PCA), partial least squares-discriminant analysis (PLS-DA) and orthogonal projection to latent structures discriminate analysis (OPLS-DA) to demonstrate comprehensive metabolic characteristics and discover differentiating metabolites. Significant changes of 11 biomarkers in rat urine were identified and they were associated with perturbations in riboflavin metabolism, arginine and proline metabolism, histidine metabolism, sphingolipid metabolism, alanine, aspartate and glutamate metabolism, cysteine and methionine metabolism and pyrimidine metabolism. Of note, MSNS administration could provide satisfactory effects on liver injury through partially reversing the level of biomarkers in the urine of liver injured rats. These results show the power of metabolomics in unraveling the potential mechanisms of MSNS and may help us to obtain a better understand of the underlying pathophysiological processes of liver injury.

Received 24th January 2013
Accepted 24th March 2013

DOI: 10.1039/c3ay40143j

www.rsc.org/methods

1 Introduction

Metabolomics, an important part of systems biology, is the global qualitative and quantitative analysis of small molecules present in biofluids.[1] It adopts a 'top-down' strategy, integrated view of biochemistry in complex organisms, as opposed to the 'bottom-up' approach that investigates network of interactions between genes, proteins and metabolites in individual cell types.[2] It can impact the whole metabolic state of an entire organism, leads to high-throughput screening in the clinical diagnosis and pharmaceutical industry,[3–7] and may also open new perspectives of assessment of the holistic efficacy of drugs. Recently, with the development of analytical technologies, chromatographic data processing, and metabolite characterization, metabolomics has brought enormous opportunities for diagnostic and pharmaceutical biomarker discovery. Ultra-performance liquid chromatography/mass spectrometry is often used in metabolomics to obtain the largest possible biochemical profile information subset[8–11] due to its excellent resolution, sensitivity and reproducibility. It can also be used to characterize, identify and quantify a great number of compounds in a biological sample where metabolite concentrations might cover a broad range of information with regard to disease pathophysiology[12–15] and potential mechanisms of drugs.[16–19]

Traditional Chinese medicine (TCM), a unique medical system with the significant characteristic of the use of multi-component drugs, can reach multiple targets with multiple components. It pursues an overall therapeutic effect in the form of combination drug formulas in an attempt to improve

[a]*College of Pharmacy, Heilongjiang University of Chinese Medicine, Harbin 150040, PR China*

[b]*Institute of Basic Medicine, Heilongjiang University of Chinese Medicine, Harbin 150040, PR China. E-mail: liukaifu86904003@yahoo.com.cn; Fax: +86 451 86345334; Tel: +86 451 86345334*

[c]*The First Affiliated Hospital, Heilongjiang University of Chinese Medicine, Harbin 150040, PR China*

† Authors contributed equally.

therapeutic efficacy.[20] Sinisan, a classical formula of TCM, was first recorded in "Shang Han Za Bing Lun" written by Zhang Zhongjing in the Han Dynasty (200–201 A.D). It is the most commonly prescribed TCM formula with the effects of protection of the hepatocyte membrane, enhancement of NO release, and dysfunction of liver infiltrating cells mainly through causing their apoptosis and has been widely used as a hepatic protectant.[21] It consists of four herbal medicines: bupleuri radix, paeoniae radix alba, aurantii fructus immaturus and glycyrrhizae radix et rhizoma.[22] For treating liver injury, Sinisan was modified by adding astragali radix, ostreae concha and xiongdan to achieve the property of soothing liver and invigorating Qi, softening hard lumps and dispelling nodes, clearing heat and detoxicating. Modified Sinisan (MSNS) has been clinically used as a common formula and produced evident effects on liver injury; however, its mechanism is still not well understood.

In the present study, a metabolomic approach based on the UPLC/ESI-Q-TOF-MS technique with pattern recognition approach and pathways analysis was employed to demonstrate the urine metabolic characteristics, identify biomarkers and speculate metabolic pathways. The aim of this study was to obtain a systematic view of mechanisms of MSNS as an effective treatment for liver injury. To our knowledge, this study is the first report of UPLC/ESI-Q-TOF-MS-based urinary metabolomics to investigate the hepatoprotective effects of MSNS.

2 Materials and methods

2.1 Chemicals and reagents

Acetonitrile (HPLC grade) was purchased from Merck (Darmstadt, Germany). Deionized water was purified with Milli-Q ultrapure water system (Millipore, Bedford, MA, USA). Formic acid (HPLC grade) was purchased from Honeywell Company (Morristown, NJ, USA). Leucine enkephalin was purchased from Sigma-Aldrich (St Louis, MO, USA). Dimethylnitrosamine (DMN) was purchased from Tianjin Chemistry Reagent Research Institution (Tianjin, China).

2.2 MSNS extract

The Chinese medicinal herbs of *Bupleurum chinense* DC., *Citrus aurantium* L., *Paeonia lactiflora* Pall., Processed *Glycyrrhiza uralensis* Fisch., *Astragalus membranaceus* (Fisch.) Bge. var. *mongholicus* (Bge.) Hsiao, *Ostrea gigas* Thunberg, xiongdan were purchased from Harbin Shiyitang Herb Store (Harbin, China). All drugs were authenticated by Prof. Xiao-Wei Du, Department of Pharmacognosy of Heilongjiang University of Chinese Medicine.

MSNS was prepared at the pharmacognosy laboratory as the following procedure: Ostreae concha (100 g) was immersed in 1900 ml water and refluxed for 30 min, then bupleuri radix (15 g), paeoniae radix alba (15 g), aurantii fructus immaturus (15 g), glycyrrhizae radix (15 g) and astragali radix (30 g) were added and refluxed for another 60 min. The solution was filtered with eight-layer gauze, and the residue was further extracted one time in the same way. The solutions of twice extractions were mixed and condensed under decompression to approximate 190 ml, and then 2 g xiongdan was added. Finally, the total solution was prepared as freeze-dried power.

2.3 Animal handing and sampling

Thirty male Wistar-derived rats (weighting 180–220 g) were provided by Good Laboratory Practice Centre of Heilongjiang University of Chinese Medicine (Harbin, China). All animals were allowed to acclimatize in metabolism cages with free access to food and tap water under the standard conditions of humidity (50% ± 10%), temperature (25 ± 2 °C) and 12 h light–dark cycle for one week prior to treatment. Animal care and all experimental procedures were conducted in accordance with the recommendations of the Guide for the Care and Use of Laboratory Animals of Heilongjiang University of Chinese Medicine. All efforts were made to ameliorate suffering of animals.

Thirty rats were randomly divided into 3 groups with 10 rats in each: the control, model and MSNS groups. The rats in the control group were administrated distilled water in the whole procedure for 28 consecutive days. The rats in the model group were injected DMN (10 mg kg^{-1} bodyweight) for 3 consecutive days each week over a period of 4 weeks.[23,24] The rats in MSNS group were injected DMN (10 mg kg^{-1} bodyweight) for 3 consecutive days per week over a period of 4 weeks and administrated MSNS (42.45 g crude drug kg^{-1} bodyweight) for 28 consecutive days. The samples of 24 h rat urine were collected on day 28. The fresh urine samples were immediately centrifuged at 3500 rpm at 4 °C for 10 min, and the supernatants were stored at −20 °C prior to analysis. The urine samples were thawed before analysis and centrifuged at 12 000 rpm at 4 °C for 10 min to remove particulate matters, then the clear supernatants were transferred to autosampler vials for UPLC/MS analysis.

2.4 UPLC conditions

The UPLC/MS analysis was performed on a Waters ACQUITY UPLC system (Waters Corporation, Milford, MA, USA) coupled with electrospray ionization (ESI) source and a Waters Micromass Q-TOF micro™ Mass Spectrometer. The separation of all samples was fulfilled with an ACQUITY UPLC BEH C_{18} column (1.7 μm, 2.1 mm × 100 mm, Waters Corp., Milford, USA) at the column temperature of 40 °C, and 3 μl of urine sample was injected into the column in each run. The flow rate was 0.4 ml min^{-1} and the mobile phase consisted of ultrapure water with 0.1% formic acid (A) and acetonitrile with 0.1% formic acid (B). The gradient program was optimized as follows: 0–8 min, 2% B to 40% B; 8–10 min, 40% B to 98% B; 10–12 min, 98% B to 2% B; 12–14 min, equilibration with 2% B. The column eluent was directed to the mass spectrometer without split. After every 8 sample injections a pooled sample followed by a blank were injected in order to ensure consistent performance of the system.

2.5 MS conditions

The mass detection was operated in positive ion mode with parameters set as follows: capillary voltage of 2700 V, sample cone voltage of 25 V, extraction cone voltage of 4 V, source temperature of 120 °C, desolvation temperature of 350 °C, cone gas flow of 50 l h^{-1} and desolvation gas flow of 750 l h^{-1}. The scan time and interscan delay were set to 0.2 and 0.02 s, respectively. Leucine-enkephalin was used as the reference compound (*m*/*z* 556.2771) at a concentration of 50 fmol l^{-1} and a flow rate of 5 μl min^{-1} *via* a lockspray interface. The mass spectrometric full-scan data were acquired from *m*/*z* 80 to *m*/*z* 1500 Da with a lockspray frequency of 10 seconds, and data averaging over 10 scans.

2.6 Data processing and multivariate data analysis

Mass spectrometry data from the UPLC/MS system were first processed with the Markerlynx Applications Manager Version 4.1 (Waters Corp., Manchester, UK) for peak detection and alignment. A table was then created including the *m*/*z* and retention time pairs with corresponding intensities for all the detected peaks from each data file in the dataset. The main parameters were set as follows: retention time range 0–10 min, mass range 80–1000 amu, and mass tolerance 0.01 Da, minimum intensity 1%, mass window 0.05, retention time window 0.20, and noise elimination level 6. The processed data were then analyzed with EZinfo software 2.0 (Waters Corp., Manchester, UK). Principal component analysis (PCA), partial least squares-discriminant analysis (PLS-DA) and orthogonal projection to latent structures discriminate analysis (OPLS-DA) in the software package were used for multivariate analysis after pareto-scaled procedure. The significance was expressed by using Student's *t*-test in SPSS 13.0 for Windows (SPSS Inc., Chicago, IL, USA). *p* values less than 0.05 were considered significant.

3 Results and discussion

3.1 Acquisition and processing of metabolic profile data

Using the optimal UPLC/ESI-Q-TOF-MS conditions described above, the typical Based Peak Intensity (BPI) profiles of whole urine samples from control and liver injury rats are shown in Fig. 1A and B, respectively. As shown in Fig. 1, the low molecular mass metabolites could be separated well in 12 minutes. After analyzing by UPLC/MS, more than 9000 ions could be detected in urine. A large number of signals obtained from the mass spectra included metabolites, adducts, ion fragments, noise and so on. In order to visualize the subtle changes among these complex datasets, multiple pattern recognition methods were utilized to phenotype their metabolome. In the present study, PLS-DA, OPLS-DA and PCA were applied to classify the metabolic phenotypes and identify biomarkers. PLS-DA, a supervised pattern recognition, which is a well-established supervised method and has been widely applied in metabolomic studies, was adopted. PLS-DA score plot showed that the urinary profile of samples obtained from the liver injury models were clearly different from control models, as shown in Fig. 2A. In the PLS-DA scores, each point represents an individual sample. Interestingly, samples subjected to the same treatment were located on the same trajectory, indicating that the treatments have disturbed the normal urine metabolic profiles of rats. The corresponding PLS-DA loading plot (Fig. 2B) showed the contribution of different variables for the differences in the model and control groups. Each triangle represented a variable and the more the variable deviates from the origin, the greater the contribution to the separation of groups. To exhibit the responsibility of each ion for these variables more intuitively, the variable importance projection (VIP)-plot and S-plot were adopted (Fig. 2C and D). Both VIP-plot and S-plot can be constructed following the OPLS-DA analysis. In the VIP-plot, each black point graph represents the value of each ion and the farther away from the origin, the higher the VIP value of the ions was. The point in VIP-value plot and the point in S-plot were in one-to-one correspondence. When VIP $\geq$ 1.0, the variable can be considered as a contributor for the classification of model and control groups. According to the result of OPLS-DA, a total of 32 variables were chosen as the potential biomarkers.

Metabolomic approach was further employed to delineate metabolic changes of liver injury after dosing MSNS. The UPLC/MS data of the MSNS-treated urinary samples were investigated using unsupervised pattern recognition (PCA) (Fig. 3), a chemometric model that reduces a matrix of data to its lowest dimension of the most significant factors. As was shown in Fig. 3, the control and model groups were significantly divided into two classes, indicating that significant biochemical changes induced by liver injury. Of note, the metabolic profile of MSNS treated group fairly differed from the model group and close to control group (Fig. 3), suggesting the deviations induced by liver injury were significantly improved after treatment of MSNS.

3.2 Biomarker characterization and hepatoprotective effects of MSNS

Identification of these metabolites was then carried out. The UPLC/MS analysis that was performed using aforesaid protocol provided the precise molecular mass, context of retention time and MS/MS data for the structural identification of biomarkers. Measurement errors of the precise molecular mass was determined within 5 ppm by Q-TOF, and in the meantime, the potential elemental composition, degree of unsaturation and fractional isotope abundance of metabolites were obtained. We searched for the presumed molecular formula in Human Metabolome Database, KEGG, Chemspider and other databases to identify the possible chemical constitutions, and MS/MS data were screened to determine the potential structures of the ions. Experiment of collision induced dissociation was also implemented to obtain fragmentation patterns of those potential biomarkers. In addition, biomarker characterization was conducted with high resolution MS and MS/MS fragments, specifically for the interpretation of the structures of

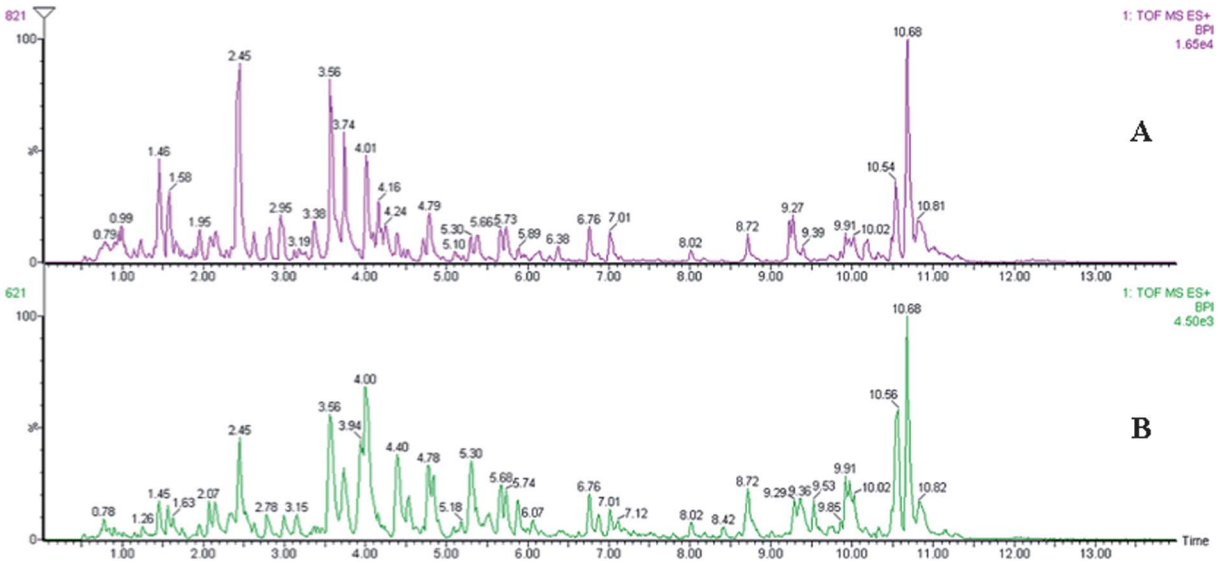

Fig. 1 The UPLC/ESI-Q-TOF-MS BPI profile of metabolome of rat urine: (A) normal rat urine, and (B) LI rat urine.

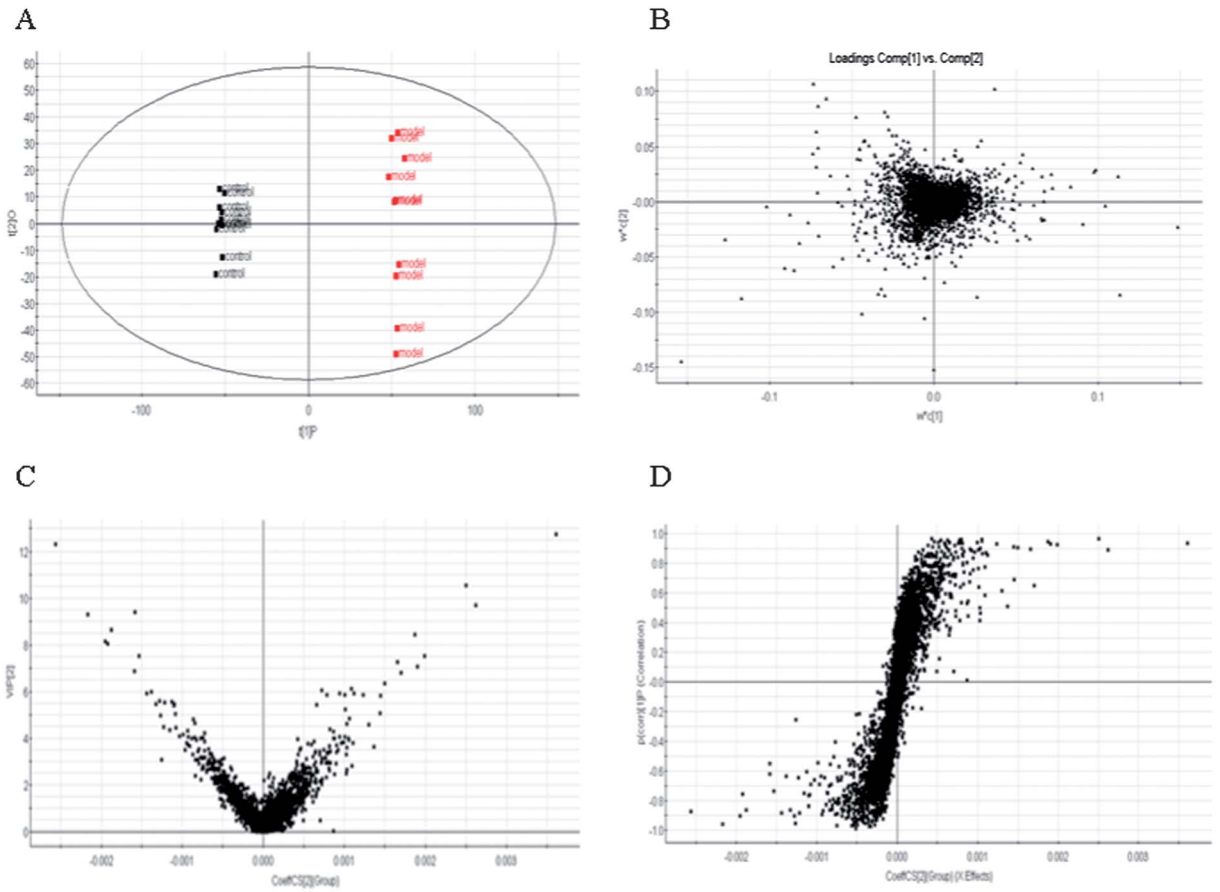

Fig. 2 (A) PLS-DA model results for control and model group. Significant metabolomic difference was shown between control and model group. One data point stands for one subject. (B) Loading plot of PLS-DA of LI. The loading plot represents the impact of the metabolites on the clustering results. PLS-DA loading plot displayed variables positively correlated with score plots. (C) VIP-value plot of control group *vs.* model group. The point graph represents the value of each metabolites. The farther away from the origin, the higher the VIP value of the metabolite was. (D) Loading S-plot of control group *vs.* model group. One point stands for one metabolite. The point in VIP-value plot and the point in S-plot were in one-to-one correspondence.

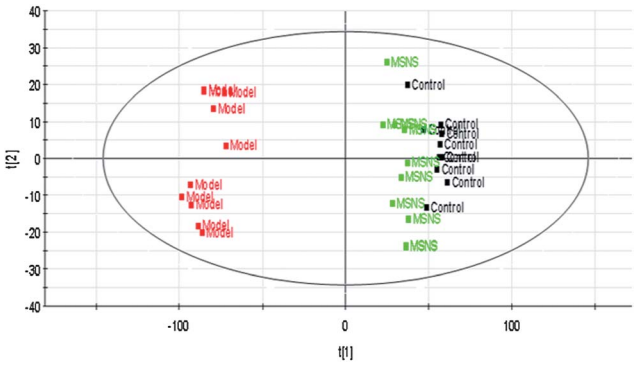

Fig. 3 Resulting scores plot from PCA of UPLC/ESI-Q-TOF-MS data obtained from control group, LI group and MSNS treatment group rat urine samples collected on day 28.

fragment ions and adducts ions. According to the protocol mentioned above, 11 endogenous metabolites were identified. Taking one ion for example, the identification procedure was as follows. One of the dominant ions *m*/*z* 162.0499 (T_R, 3.57 min) has a high VIP value. This ion might contain an odd number of nitrogen atoms because its precise molecular weight was 161.0324. Elemental composition of this ion were speculated as $C_5H_7NO_5$ using MarkerLynx. The main fragment ions analyzed by MS/MS screening were *m*/*z* 128, 116 and 89, which could correspond to lost $-H_2O_2$, $-CH_2O_2$ and $-C_2H_3NO_2$, respectively. Finally, it was speculated as 4-hydroxy-L-glutamic acid when researched in databases mentioned above. Its mass spectrum and proposed fragmentation pathway are displayed in Fig. 4. All the biomarkers identified are shown in Table 1.

By comparison of the ion intensity of potential biomarkers between model group and control group, five metabolites, formiminoglutamic acid, dihydroceramide, 4-hydroxy-L-glutamic acid, 2-keto-glutaramic acid and 1-pyrroline-4-hydroxy-2-carboxylate were up-regulated and riboflavin, thiocysteine, hippuric acid, uridine, *N*1-(alpha-D-ribosyl)-5,6-dimethylbenzimidazole and 4-guanidinobutanoic acid were down-regulated by liver injury stimulus (Table 1). Additionally, in order to characterize the effects of MSNS more clearly, the intensity level of 11 biomarkers in the different groups was analyzed (Table 1 and Fig. 5). Results showed that intensity of all biomarkers identified in MSNS group indicating the tendency to correct the derivations. Moreover MSNS could reverse the level of most biomarkers (except riboflavin, thiocysteine and uridine) in the urine of liver injury rats, which might suggest that MSNS had extensive effects in the treatment of liver injury.

3.3 Biological pathway analysis and dynamic changes of biomarkers

Metabolic pathway analysis was performed to analyzing global metabolomics in order to characterize the phenotypically biochemical perturbations using MetPA. MetPA, a web-based metabolomics tool for pathway analysis, based the high-quality KEGG metabolic pathways as the backend knowledgebase and integrates novel algorithms and concepts and well-established methods into pathway analysis.[25,26] Metabolic pathway analysis revealed that biomarkers identified are important for the host response to liver injury and are responsible for riboflavin metabolism, arginine and proline metabolism, histidine metabolism, sphingolipid metabolism, alanine, aspartate and glutamate metabolism, cysteine and methionine metabolism and pyrimidine metabolism (Fig. 6 and Table 2). The detailed construction of the altered sphingolipid metabolism pathways (Fig. 7) with higher score in rats was generated using reference map by searching KEGG. Of the distinct metabolites from these pathways, many are in various stages of progress of liver injury. Some significantly changed metabolites like 4-guanidinobutanoic acid and 1-pyrroline-4-hydroxy-2-carboxylate have been used to explain the arginine and proline metabolism, and *N*1-(alpha-D-ribosyl)-5,

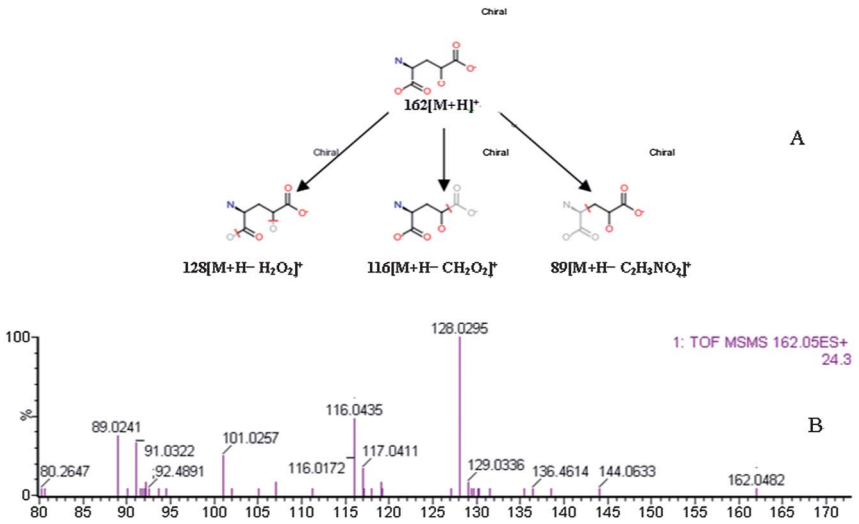

Fig. 4 (A) Proposed fragmentation pathway of 4-hydroxy-L-glutamic acid. (B) Mass spectra of 4-hydroxy-L-glutamic acid.

Table 1 Metabolites selected as biomarkers characterized in urine profile and their change trends ($n = 10$ in each group)[a]

No.	VIP	Observed $[M + H]^+$	Rt	Actual-M	Proposed compound	Proposed structure	Trend in model group[b]	Trend in MSNS group[c]
1	4.04	377.1368	4.00	376.1383	Riboflavin	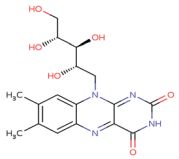	↓***	↑
2	4.06	175.1188	4.16	174.0641	Formiminoglutamic acid	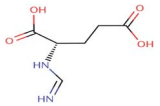	↑*	↓*
3	4.43	154.0467	1.64	152.9918	Thiocysteine	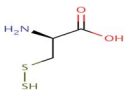	↓***	↑
4	4.48	279.1273	4.16	278.1266	*N*1-(alpha-D-ribosyl)-5,6-dimethyl-benzimidazole	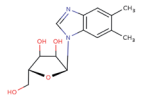	↓***	↑***
5	4.59	330.3340	10.15	329.2930	Dihydroceramide		↑***	↓***
6	5.24	146.0535	4.84	145.0375	2-Keto-glutaramic acid	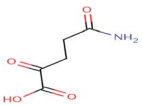	↑**	↓***
7	5.45	245.1574	1.49	244.0695	Uridine	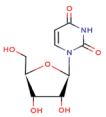	↓***	↑
8	5.54	146.0886	0.97	145.0851	4-Guanidinobutanoic acid	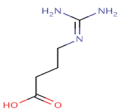	↓***	↑***
9	7.51	130.0591	4.79	129.0426	1-Pyrroline-4-hydroxy-2-carboxylate		↑***	↓***
10	9.31	180.0605	3.74	179.0582	Hippuric acid	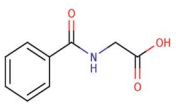	↓***	↑***
11	9.69	162.0499	3.57	161.0324	4-Hydroxy-L-glutamic acid	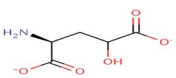	↑***	↓***

[a] Levels of potential biomarkers were labeled with (↓) down-regulated and (↑) up-regulated (*$p < 0.05$; **$p < 0.01$; ***$p < 0.001$). [b] Change trend compared with control group. [c] Change trend compared with model group.

6-dimethyl-benzimidazole and riboflavin have been used to explain the riboflavin metabolism. As a result, the 7 metabolic pathways show marked perturbations over the entire time-course of liver injury and could contribute to the development of liver injury. At the same time, metabolomic feature network demonstrated that MSNS shows hepatoprotective effects by reversing metabolites towards control levels, especially for the metabolites in the perturbed pathways.

Further analysis revealed that biomarkers identified together are important for the response to liver injury. Riboflavin is an easily absorbed, water-soluble micronutrient with a key role in maintaining human health. As one of the family of B vitamins, riboflavin contributes to cellular growth, enzyme function, and energy production. Vitamin B_2 is also required for red blood cell formation and respiration, antibody production, and for regulating human growth and reproduction. It is essential for healthy skin, nails, hair growth and general good health, including regulating thyroid activity. Riboflavin functions as the precursor for flavin mononucleotide (FMN) and flavin adenine dinucleotide (FAD).[27] FAD is a cofactor in many reactions of intermediary

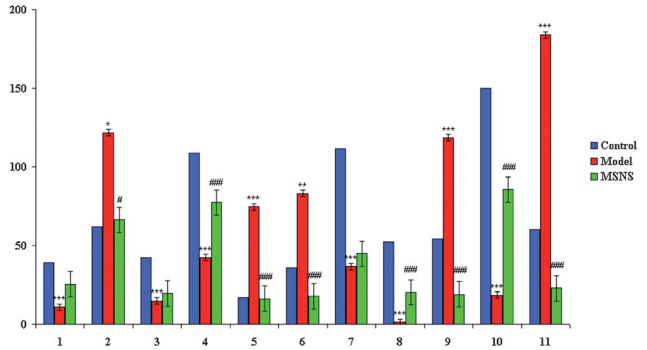

Fig. 5 Differential expression levels (mean) of biomarkers in different groups. The corresponding markers are represented in Table 1. Student's *t*-test was used to determine the significance of the change in relative intensity for each metabolite. Bars represent the mean relative metabolite concentration. Compare with control group: $^{*}p < 0.05$, $^{**}p < 0.01$, $^{***}p < 0.001$; compare with model group: $^{\#}p < 0.05$, $^{\#\#}p < 0.01$, $^{\#\#\#}p < 0.001$.

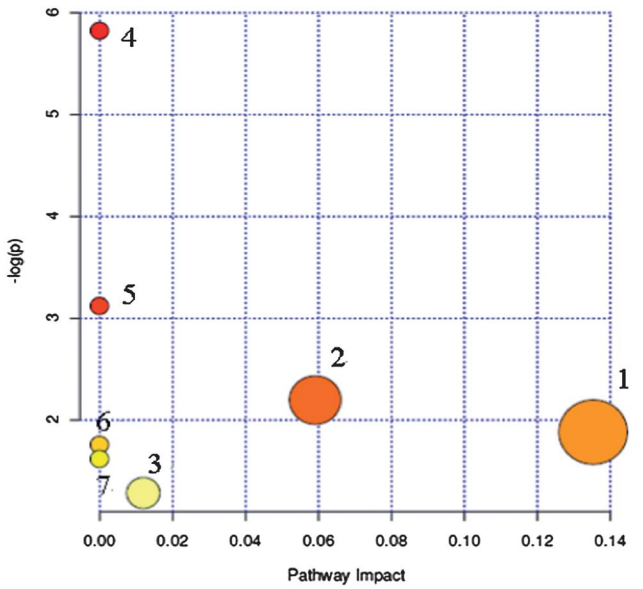

Fig. 6 Summary of pathway analysis with MetPA. (1) Sphingolipid metabolism; (2) histidine metabolism; (3) pyrimidine metabolism; (4) riboflavin metabolism; (5) arginine and proline metabolism; (6) alanine, aspartate and glutamate metabolism; (7) cysteine and methionine metabolism.

metabolism, such as carbohydrate, fat, and amino acid synthesis. FAD and R5P are also necessary for the activation of other vitamins and enzyme systems. Folate and pyridoxine are vitamins that rely on riboflavin for activation. FMN and FAD act as hydrogen carrier to produce ATP through metabolism of carbohydrates and fats. Riboflavin has been claimed to have a protective effect on the liver. So, riboflavin might be useful biomarker for liver injury. Hippuric acid (HA) is an acyl glycine biosynthesized from glycine, benzoic acid and CoA by enzymes located in the mitochondrial matrix of liver cells. As a biomarker in urine of liver injury rats, the content of hippuric acid decreased. This is consistent with the results in our research. Uridine, a uracil nucleoside, is an essential component of RNA synthesis and plays an important role in the synthesis of glycogen. In addition, it contributes to the synthesis of bio-membranes through formation of pyrimidine–lipid conjugates. Uridine has been reported to have other physiological actions in animals' studies, such as a vasoconstrictive effect in rats, which was reversed by adenosine, and hyperpolarized amphibian ganglia and superior cervical ganglia in rats, possibly related to an inhibitory activity. In particular, uridine supplemental therapy can restore both liver growth and hepatocyte proliferation,[28] so uridine might be another biomarker for liver injury.

Formiminoglutamic acid (FIGLU) is an intermediate metabolite in the degradation of histidine. In the presence of tetrahydrofolic acid, the formimino group is transferred from FIGLU to the tetrahydrofolic acid which is thus converted to 5-formiminotetrahydrofolic acid. This conversion apparently is facilitated by the enzyme FIGLU transferase. 5-Formiminotetrahydrofolic acid is then converted by a series of reactions to 10-formyltetrahydrofolic acid, a labile, highly active compound in formyl transfer reactions. If tetrahydrofolic acid is not present, which is the case in folic-acid-deficient subjects, this transfer of the formimino group cannot take place, and FIGLU is then excreted in the urine. Formiminoglutamic acid has been found in the urine of the majority of patients with liver disease. Thus, FIGLU might be sensitive indicator biomarker of liver injury. However, other biomarkers were warranted the further mechanistic exploration of this formula.

Table 2 Result from pathway analysis with MetPA[a]

No.	Pathway name	Total	Expected	Hits	Raw *p*	−log(*p*)	Impact
1	Sphingolipid metabolism	21	0.16	1	1.53×10^{-1}	1.87×10	0.14
2	Histidine metabolism	15	0.12	1	1.12×10^{-1}	2.19×10	0.06
3	Pyrimidine metabolism	41	0.32	1	2.79×10^{-1}	1.28×10	0.01
4	Riboflavin metabolism	11	0.09	2	2.96×10^{-3}	5.82×10	0.00
5	Arginine and proline metabolism	44	0.35	2	4.42×10^{-2}	3.12×10	0.00
6	Alanine, aspartate and glutamate metabolism	24	0.19	1	1.74×10^{-1}	1.75×10	0.00
7	Cysteine and methionine metabolism	28	0.22	1	2.00×10^{-1}	1.61×10	0.00

[a] Note: total is the total number of compounds in the pathway; the hits is the actually matched number from the user uploaded data; the raw *p* is the original *p* value calculated from the enrichment analysis; the impact is the pathway impact value calculated from pathway topology analysis.

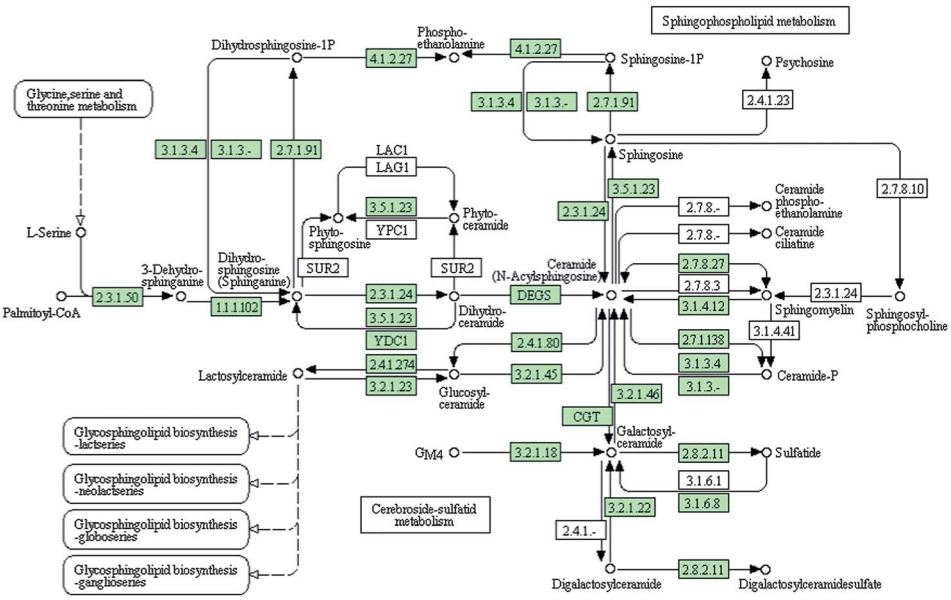

Fig. 7 Construction of the sphingolipid metabolism pathway in rats. The map was generated using the reference map by KEGG (http://www.genome.jp/kegg/). The green boxes: enzymatic activities with putative cases of analogy in rats.

4 Conclusion

Metabolomics has brought enormous opportunities for biomarker discovery and potential mechanisms research of TCM. In this study, a metabolomic approach based on UPLC/ESI-Q-TOF-MS detection, pattern recognition analyses and metabolic pathway analysis has been successfully established for biomarkers exploration in liver injury and mechanism studies of MSNS. This is the first demonstration of metabolomic approach to show metabolic changes in liver injury after dosing MSNS regiment treatment. Eleven potential biomarkers of significant contribution were preliminary identified and the perturbations in those metabolites were associated with riboflavin metabolism, arginine and proline metabolism, histidine metabolism, sphingolipid metabolism, alanine, aspartate and glutamate metabolism, cysteine and methionine metabolism and pyrimidine metabolism. Of note, MSNS administration could provide satisfactory effects on liver injury through partially reversing the level of biomarkers in the urine of liver injury rats and regulating the multiple perturbed pathways. Altogether, the importance of metabolomics as a powerful tool for discovering drug targets and providing insights into mechanisms of drugs is highlighted once more.

Acknowledgements

This work was financially supported by the Natural Science Foundation of Heilongjiang Province (D201037), Heilongjiang Provincial Administration of Chinese Medicine Project (ZHY10-Z47), Heilongjiang Postdoctoral Fund (LBH-Z09010), Heilongjiang University of Chinese Medicine Research Fund (200909).

References

1 J. K. Nicholson and I. D. Wilson, *Nat. Rev.*, 2003, **2**, 668–676.
2 J. K. Nicholson and J. C. Lindon, *Nature*, 2008, **455**, 1054–1056.
3 A. Sreekumar, L. M. Poisson, T. M. Rajendiran, A. P. Khan, Q. Cao, J. Yu, B. Laxman, R. Mehra, R. J. Lonigro, Y. Li, M. K. Nyati, A. Ahsan, S. Kalyana-Sundaram, B. Han, X. Cao, J. Byun, G. S. Omenn, D. Ghosh, S. Pennathur, D. C. Alexander, A. Berger, J. R. Shuster, J. T. Wei, S. Varambally, C. Beecher and A. M. Chinnaiyan, *Nature*, 2009, **457**, 910–914.
4 I. R. Lanza, S. Zhang, L. E. Ward, H. Karakelides, D. Raftery and K. S. Nair, *PLoS One*, 2010, **5**, e10538.
5 G. S. Catchpole, M. Beckmann, D. P. Enot, M. Mondhe, B. Zywicki, J. Taylor, N. Hardy, A. Smith, R. D. King, D. B. Kell, O. Fiehn and J. Draper, *Proc. Natl. Acad. Sci. U. S. A.*, 2005, **102**, 14458–14462.
6 D. G. Robertson, M. D. Reily and J. D. Baker, *J. Proteome Res.*, 2007, **6**, 526–539.
7 A. H. Zhang, H. Sun, Z. G. Wang, W. J. Sun, P. Wang and X. J. Wang, *Planta Med.*, 2010, **76**, 2026–2035.
8 X. J. Wang, H. Sun, A. H. Zhang, P. Wang and Y. Han, *J. Sep. Sci.*, 2011, **34**, 3451–3459.
9 H. G. Gika, G. A. Theodoridis, M. Earll, R. W. Snyder, S. J. Sumner and I. D. Wilson, *Anal. Chem.*, 2010, **82**, 8226–8234.
10 A. H. Zhang, H. Sun and X. J. Wang, *Hepatology*, 2012, DOI: 10.1002/hep.26130.
11 A. H. Zhang, H. Sun, P. Wang, Y. Han and X. J. Wang, *Analyst*, 2012, **137**, 293–300.
12 V. V. Tolstikov, O. Fiehn and N. Tanaka, *Methods Mol. Biol.*, 2007, **358**, 141–155.
13 D. Field, S. A. Sansone, A. Collis, T. Booth, P. Dukes, S. K. Gregurick, K. Kennedy, P. Kolar, E. Kolker, M. Maxon, S. Millard, A. M. Mugabushaka, N. Perrin, J. E. Remacle, K. Remington, P. Rocca-Serra, C. F. Taylor, M. Thorley, B. Tiwari and J. Wilbanks, *Science*, 2009, **326**, 234–236.

14 O. Fiehn, *Trends Anal. Chem.*, 2008, **27**, 261–269.
15 X. J. Wang, A. H. Zhang, Y. Han, P. Wang, H. Sun, G. C. Song, T. W. Dong, Y. Yuan, X. X. Yuan, M. Zhang, N. Xie, H. Zhang, H. Dong and W. Dong, *Mol. Cell. Proteomics*, 2012, **11**, 370–380.
16 B. Yang, A. H. Zhang, H. Sun, W. Dong, G. L. Yan, T. L. Li and X. J. Wang, *J. Pharm. Biomed. Anal.*, 2012, **58**, 113–124.
17 X. P. Liang, X. Chen, Q. L. Liang, H. Y. Zhang, P. Hu, Y. M. Wang and G. A. Luo, *J. Proteome Res.*, 2011, **10**, 790–799.
18 P. Jiang, W. X. Dai, S. K. Yan, Z. L. Chen, R. L. Xu, J. M. Ding, L. Xiang, S. P. Wang, R. H. Liu and W. D. Zhang, *Mol. BioSyst.*, 2011, **7**, 824–831.
19 X. J. Wang, A. H. Zhang and H. Sun, *OMICS: J. Integr. Biol.*, 2012, **16**, 414–421.
20 L. Wang, G. B. Zhou, P. Liu, J. H. Song, Y. Liang, X. J. Yan, F. Xu, B. S. Wang, J. H. Mao, Z. X. Shen, S. J. Chen and Z. Chen, *Proc. Natl. Acad. Sci. U. S. A.*, 2008, **105**, 4826–4831.
21 Y. T. Wang, Q. R. Tan, L. L. Sun, J. Cao, K. F. Dou, B. Xia and W. Wang, *Neurosci. Lett.*, 2009, **449**, 215–219.
22 J. Y. Jiang, C. X. Zhou and Q. Xu, *Biol. Pharm. Bull.*, 2003, **26**, 1089–1094.
23 J. George, K. R. Rao, R. Stern and G. Chandrakasan, *Toxicology*, 2001, **156**, 129–138.
24 Y. L. Jin, H. Enzan, N. Kuroda, Y. Hayashi, M. Toi, E. Miyazaki, T. Hamauzu, M. Hiroi, L. M. Guo, Z. S. Shen and T. Saibara, *Med. Mol. Morphol.*, 2006, **39**, 33–43.
25 X. J. Wang, B. Yang, A. H. Zhang, H. Sun and G. L. Yan, *J. Proteomics*, 2012, **75**, 1411–1427.
26 X. J. Wang, Q. Q. Wang, A. H. Zhang, F. M. Zhang, H. Zhang, H. Sun, H. X. Cao and H. M. Zhang, *J. Pharm. Biomed. Anal.*, 2013, **74**, 22–30.
27 I. Hassan, S. Chibber, A. A. Khan and I. Naseem, *PLoS One*, 2012, **7**, e36273.
28 A. R. Biglarnia, T. Lorant, H. S. Lee, G. Tufveson, M. Ttsch and M. Malag, *Hepatol. Res.*, 2009, **39**, 86–92.